INTERMETALLIC GROWTH OF Cu_6Sn_5 AS A FUNCTION OF CU CRYSTALLOGRAPHIC ORIENTATION

by

Ziyun Huang

A Thesis

Submitted to the Faculty of Purdue University

In Partial Fulfillment of the Requirements for the degree of

Master of Science in Materials Engineering

School of Materials Engineering

West Lafayette, Indiana

August 2021

THE PURDUE UNIVERSITY GRADUATE SCHOOL
STATEMENT OF COMMITTEE APPROVAL

Dr. John Blendell, Co-chair
School of Materials Engineering

Dr. Carol Handwerker, Co-chair
School of Materials Engineering

Dr. Eric Kvam
School of Materials Engineering

Approved by:
Dr. David Bahr

Dedicated to my family for their selfless support

ACKNOWLEDGMENTS

I would like to thank, from the depth of my heart, to both of my supervisors and committee members for their guidance and support through the last three years. Looking back at the notes and presentation I made when I first started the graduate project, I am always amazed at how much I have grown. It will never happen without your help. I am blessed to have all my great friends as well who continuously encourages me. Living far away from home is not easy, and thank for all of you who help brighten my life. I also want to thank my family for their love and support all these years. Due to pandemic they are not able to attend my graduation, but I am sure they will be proud of me, and I will try my best to keep them proud in the future.

Lastly I want to express my gratitude to my boyfriend Juncheng and my cat Jiu. Together you have accompanied so many unforgettable moments with me, and I hope I can repay this love and trust.

TABLE OF CONTENTS

ABSTRACT

The morphologies and growth behavior of Cu_6Sn_5 intermetallic compound (IMC) formed between Sn-based solder and large-grain polycrystalline Cu substrate were systematically investigated. Hexagonal Cu_6Sn_5 grains were observed to form at certain reflow condition, which matches well with the literature results for IMC growing on single crystal substrate. The kinetics of IMC growth was also investigated and different mechanisms were proposed for different evolution stages. It was observed that facet formation should be a growth shape rather than an equilibrium shape, and the orientation relationship between Cu and Cu_6Sn_5 was studied using scanning electron microscope (SEM) and Electron backscatter diffraction (EBSD), and were visualized on inverse pole figure.

1. INTRODUCTION

1.1 Solder system and under-bump metallization (UBM)

Lead-containing solder alloy has been playing an important part in electronic industry for the last several decades, and has advantages of low melting point, good wettability on many substrates (Cu, Ag, Pb, Au etc), good mechanical properties and low cost. However, regardless of all advantages Pb-containing solders have, they are replaced gradually by lead-free solders due to the detrimental effect of Pb to environment. With the enactment of RoHS regulations, it is a trend in present industry to move to Pb-free production. Sn-based solders are promising lead-free candidates due to their low melting points. In lead-free solder cases, Sn is the main active component and reacts with UBM to form intermetallic compound (IMC).

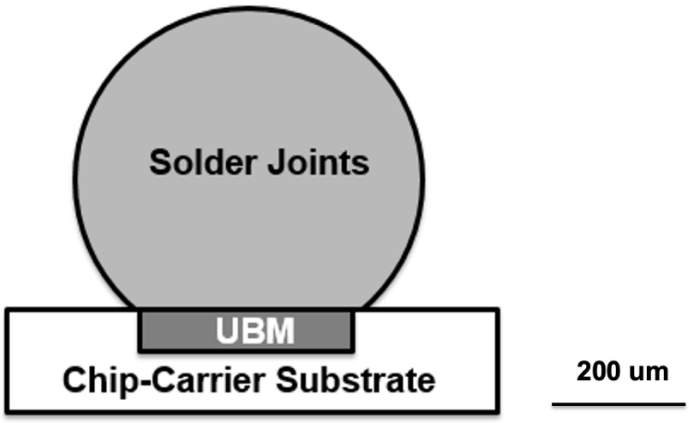

Fig. 1 a schematic diagram of solder system and under-bump metallization. A scale bar is introduced to show the size of solder joints

Fig. 1 is a schematic diagram of solder structure. The substrate dissolves into molten solder immediately after flux removes substrate metal oxides and allows solder/metal contact. Then in less than a second, solder near the interface becomes supersaturated with the dissolved metal and IMC formation would take place. The metastable solubility is about 2-3 times larger than the stable one and indicates the metal dissolution rate into molten solder [1]. The formation of a continuous IMC layer reduces interfacial energy and is a sign of good bonding and good wettability [2]. But IMC usually is mechanically fragile, and brittleness of thin IMC layer will have great impact on the overall mechanical performance as solder volume shrinks. So the

control of IMC growth becomes a great concern of present researchers, and considerable time and energy have been spent on the study of IMC evolution during reflowing.

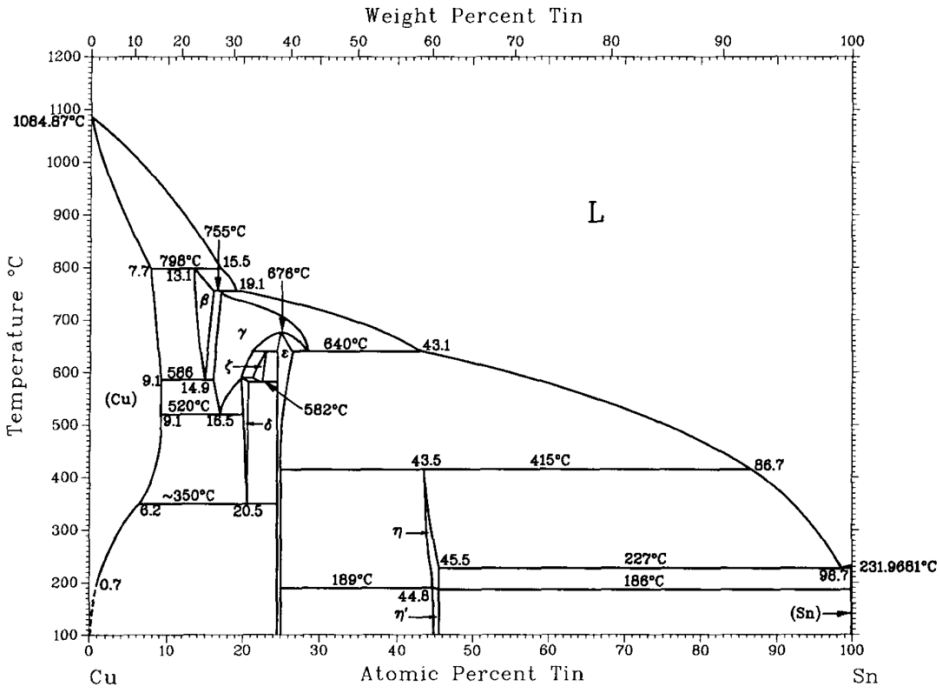

Fig. 2 Cu-Sn phase diagram [3]

Copper is the most commonly used metal pad under solder bump, and reacts with Sn-based solder to form Cu_6Sn_5 (η/η' phase) and Cu_3Sn (ε phase) as shown in the phase diagram above. Cu_6Sn_5 layer is formed first at solder/substrate interface and Cu_3Sn is then formed between Cu_6Sn_5 and copper after certain incubation time. Cu_6Sn_5 usually has a faster growth rate especially during the early stages, and has developed various morphology during heat treatment. It is generally acknowledged that Cu_6Sn_5 exhibits two crystal structures, with a transformation temperature at ~189 °C from hexagonal η- Cu_6Sn_5 to monoclinic η′- Cu_6Sn_5. A TTT diagram was developed for the transformation, and at regular cooling rate only hexagonal η- Cu_6Sn_5 is formed[4]. It is also observed that the monoclinic η′- Cu_6Sn_5 has a strong pseudo-hexagonal symmetry that it is hard to tell apart the two structures from XRD patterns. Therefore the following discussions will be based on η phase Cu_6Sn_5 unless particularly pointed out.

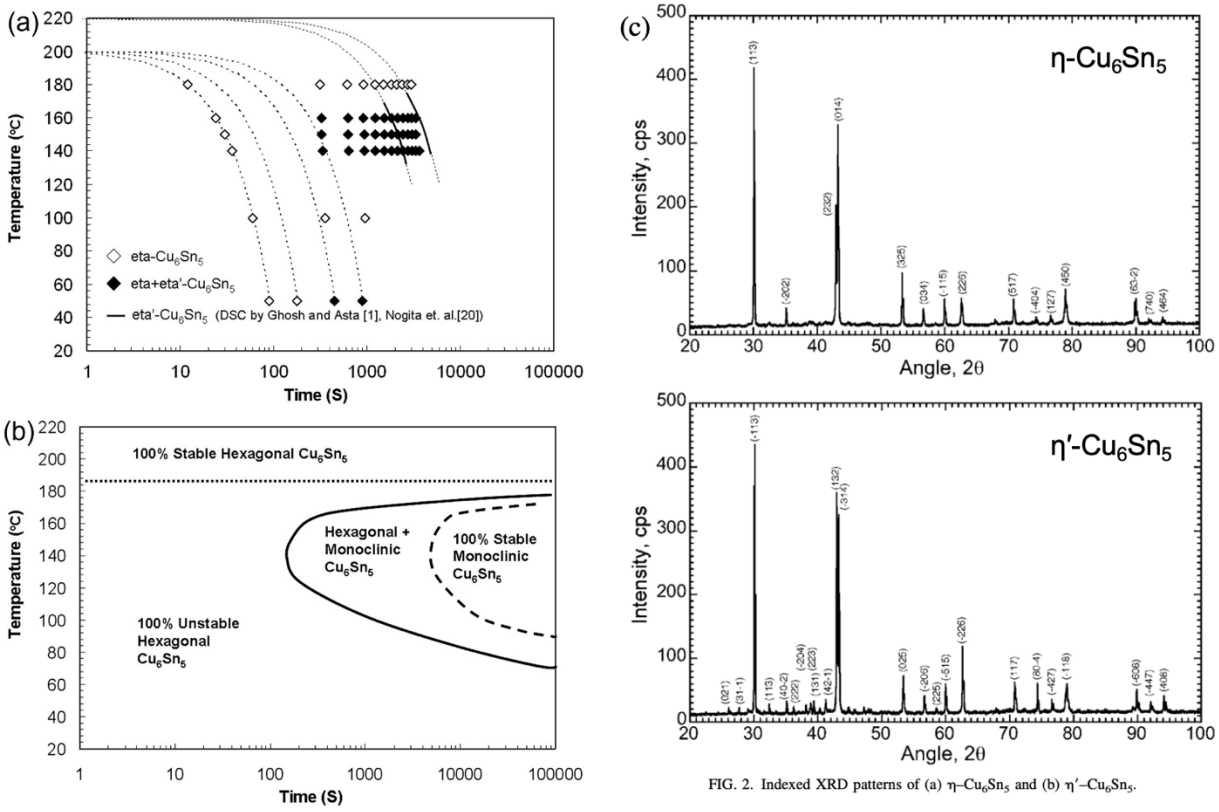

FIG. 2. Indexed XRD patterns of (a) η–Cu_6Sn_5 and (b) η′–Cu_6Sn_5.

Fig. 3 (a) A graphical summary of the experimental conditions and phases tested. (b) time-temperature-transformation (TTT) diagram for two Cu_6Sn_5 phases [4] (c) standard XRD patterns of η and η' phases from PDF cards

1.2 Different evolution stages in Cu_6Sn_5

IMC evolution can be categorized into several stages and different mechanisms were proposed to describe each stage. Cu dissolution started immediately after solder contacting metal substrate, and after a short period of time, the solder layer adjacent to Cu substrate became supersaturated and lead to IMC nucleation. The dissolution rate was determined by metastable solubility ${}^{m}x_{Cu}$, which is 2-3 times higher than the stable one, and indicated the maximum amount of Cu that can dissolve in solder without precipitating back. The saturation limit as well as the metastable solubility can be obtained in Gibbs free energy plots as Fig.4, and can be easily found in many databases [1]. Kivilahti et al have calculated the Gibbs free energy for Cu-Sn system and found the metastable solubility ${}^{m}x_{Cu}$ close to 10% at 235°C by

drawing the common tangent line. The large solubility indicated large driving force for fast Cu dissolution and consequent IMC growth[1]. When molten solder reacts with Cu substrate, the first stage is Cu dissolution, until solder becomes supersaturated and the metastable solubility is reached. Then the continuous dissolution of Cu will precipitate back and Cu concentration near the interface will stop increasing.

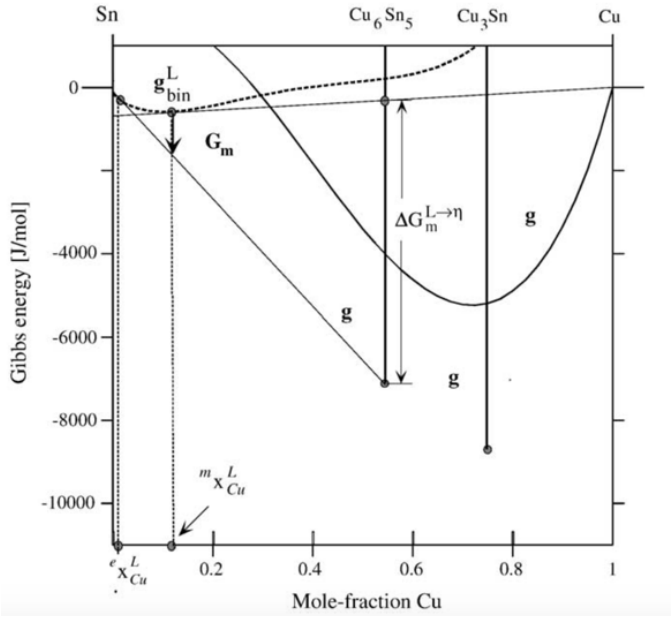

Fig. 4 Gibbs free energy diagram of Sn–Cu system at 235ºC [1]. The metastable solubility of Cu in molten Sn is denoted by ${}^{m}x_{Cu}{}^{L}$, which is determined by the common tangent line between molten Sn and Cu6Sn5, the first IMC to form

After Cu supersaturation and Cu_6Sn_5 nucleation, IMC grains began to form a relative continuous layer at solder/substrate interface. It was generally accepted that diffusion rate has a great influence on IMC morphology, and the sufficient and necessary conditions for scallop-type Cu_6Sn_5 formation is complete wetting condition as well as a sufficiently small diffusivity ratio D_{GB}/D_L, while D as the diffusivity along grain boundary (GB) and in molten solder respectively. If any one of these conditions is not met, the scallop-type Cu_6Sn_5 would change to a layer-type one [5]. If D_{GB}/D_L is not small enough, the fast grain boundary diffusion will induces higher growth rates, preventing the grain boundaries being wetted completely even if it would have a smaller interfacial energy [6] . Detailed discussion of morphology will be presented in later section.

At an adequate aging time the Cu_6Sn_5 grains coarsened and showed scalloped morphology. Tu et al proposed a flux-driven ripening (FDR) theory for Cu_6Sn_5 coarsening in molten solders, in which diffusion happened completely along liquid channels. The grains are assumed to grow in a self-similar manner, and aspect ratio is constant between perpendicular length and lateral width. The improvement for FDR theory is that it doesn't require a closed system, and growth was calculated as a 1/3 power law in time ($d - d_0 = kt^{1/3}$), similar to classical LSW ripening theory but with a modified grain size distribution. [7,8]

To sum up, initially when Cu_6Sn_5 layer was very thin, the diffusion distance of Sn and Cu atoms to react with each other was very short, and diffusion happened almost instantaneously compared to Cu/Sn reaction. The growth of Cu_6Sn_5 is therefore considered as having linear kinetics (growth exponent n = 1). As Cu_6Sn_5 layer formed continuously at interface, IMC growth became more and more dependent on diffusion through IMC layer, and the effect of chemical reaction gradually decreased and became less significant. At this stage, n = 0.5 and IMC growth was considered as diffusion-controlled. After long enough time, grain boundary diffusion, interface diffusion, grain coarsening and dissolution have all occurred, and n could be smaller than 0.5.

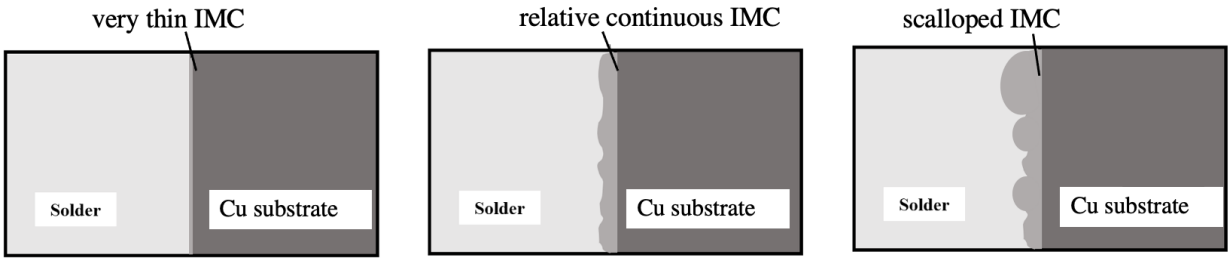

Fig. 5 A diagram showing different stages in IMC growth

1.3 Faceting in Cu_6Sn_5

Researchers have observed various morphologies in Cu_6Sn_5 such as scallops[8-11], plates [11], needles[12], hollow rods[13] , and dendrites [13]. Scallop-type Cu_6Sn_5 grains are most commonly observed, but the scallop morphology was dependent to solder composition, heat

treatment temperature and substrate. For SnPb solders, Cu_6Sn_5 became more faceted when composition was further away from the eutectic composition with higher Sn percentage, and more rounded when composition got closer to the Pb side. The scallop-to-facets transition has also been noticed for other solders. Yang et al found out that for Sn3.5Ag solder, faceted IMCs began to form when reflowing temperature was higher than 543K, and scallop type IMCs were formed reflowed at a temperature lower than 533K [11].

More interestingly, the two morphologies could be transformed into each other as long as the corresponding reflow condition changed, both for eutectic SnPb solder and Sn3.5Ag solder. During solid state aging scallop Cu_6Sn_5 would transform to layered type, and would transform back to scallop-type morphology once wetted by molten solder [11,14]. Yang et al pointed out that the morphology change is caused by temperature rather than higher Cu content in molten solder by strongly stirred the melt. The morphology transition was explained by the dependence of Jackson's parameter on temperature. Based on the classical unary solidification theory, Jackson's parameter of crystals with rough surfaces is smaller than 2 while it is larger than 2 for faceted grains [15,16].

To explain the relationship between Jackson's parameter and grain morphology, assume there are overall N sites at solid-liquid interface during the solidification process, and n of them are occupied, then x = n/N is the occupation fraction. Atoms jumping from liquid onto solid will lead to an energy change $\Delta G = \Delta H - T\Delta S = \Delta U + p\Delta V - T\Delta S = \Delta U - T\Delta S$. ΔU can be expressed as $\Delta U = \frac{1}{2}\mathrm{N}(1-\mathrm{x})\mathrm{Z}' * \mathrm{x} * 2\frac{\Delta \mathrm{H}}{Z}$, where Z' and Z are the number of nearest neighborhood at the interface and in the bulk crystal respectively. $2\frac{\Delta \mathrm{H}}{Z}$ is the energy to break one bond, and $\frac{1}{2}\mathrm{N}(1-\mathrm{x})\mathrm{Z}'$ corresponds to the number of bonds that are broken to form N(1-x) vacancies. The energy change relationship can be translated into $\Delta U = x(1-x) * \alpha * RT$, where α is defined as Jackson's parameter. By definition, $\alpha = \frac{\Delta \mathrm{H}}{RT} * \frac{\mathrm{Z}'}{Z}$. Therefore, ΔG can be rewritten as

$$\Delta \mathrm{G} = \mathrm{x}(1-\mathrm{x}) * \alpha * \mathrm{RT} + \mathrm{RT}[\mathrm{xlnx} + (1-\mathrm{x})\ln(1-\mathrm{x})]$$

As shown in Fig. 6, the Gibbs free energy is shown as a function of x, and the plot has two distinct shapes: one has the minimum point at x=0.5 as the bottom curve, and the other has two minimum points (x close to 0 and x close to 1) as the top curve [17] . When Jackson's parameter is larger than 2 (usually larger than 5 to show the morphological difference), the curve has the shape that free energy minimum at x close to 0 or 1; when smaller than 2, the minimum at 0.5. In the former case there are few atoms or vacancies at the interface, and the interface therefore is crystallographic smooth and macroscopically faceted. As Jackson's parameter is dependent on free energy, which could be expressed as a function of temperature, Jackson's parameter will change at a different temperature. The parameter can serve as a sign of different interfacial energy and lead to a different morphology.

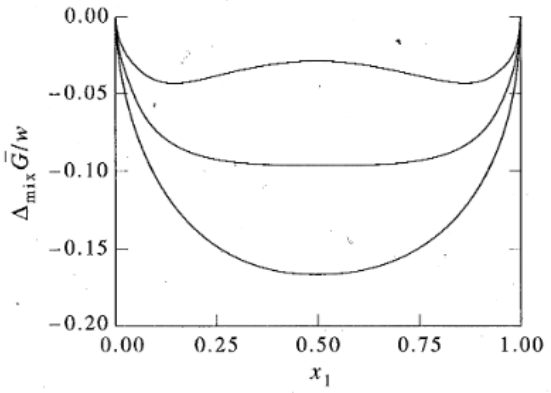

Fig. 6 Gibbs free energy at different fraction x. The top curve has two local minimums close to x = 0 and x = 1 respectively, and the bottom curve has a single minimum at x = 0.5. The middle curve doesn't have an obvious minimum as a transition state [17] .

The morphology transition can also be observed by changing cooling rate and Cu content in solders. Cu_6Sn_5 exhibited a rods-to-dendrites transition with increased cooling rate in higher Cu content solders [13]. The transition was explained as the higher Cu content and higher cooling rate increased the local concentration in molten solder and therefore lead to interface roughening. An interesting fact observed is that Cu_6Sn_5 rod is hollow when cooling rate is quite slow (~0.03 K/s), which may result from the wetting of dislocation core by molten solder or remelt of dislocation core due to high strain energy. Another factor affecting the morphology is additive elements in solder. As discussed above, for Sn3.5 Ag solder the condition of faceted Cu_6Sn_5 formation is when reflow temperature is higher than 543k, but researchers found out that for Sn3.5Ag0.1Ni and Sn3.5Ag0.1Co solders, the IMCs remained faceted at 523K [18].

The stabilizing effect of Ni has been noticed by Nogita et al as well, as the hexagonal structure of Cu_6Sn_5 is stable down to room temperature even with trace Ni additions (Sn-0.7wt%Cu-0.05wt%Ni) [19].

Similar to cooling rate, heat treatment time can lead to a shape transition as well. Zou et al found out that at 260 °C, there was a facet-to-scallop transition at longer reflow time [18]. Fig.7 is an example on (111) single crystal Cu. It is clearly seen that at 320s Cu_6Sn_5 scallops started to form at the top left corner, and at 600s almost all prism-like Cu_6Sn_5 have turned into scallops . The morphology change indicates that Cu_6Sn_5 facets are more likely to be the growth shape rather than equilibrium shape, as facets are eventually replaced by scallops. The difference between growth shape and equilibrium shape are often neglected by researchers, and the concepts are often misused. The key difference is that equilibrium shape, as the name indicates, shows anisotropy of surface energy and is the structure shown in equilibrium, while growth shape shows difference in growth rate in different directions and is a “kinetic structure”. Based on the morphological transition shown in Fig.7, it is easy to tell that the morphological anisotropy in Cu_6Sn_5 facets is caused by difference in growth rate and is a growth shape.

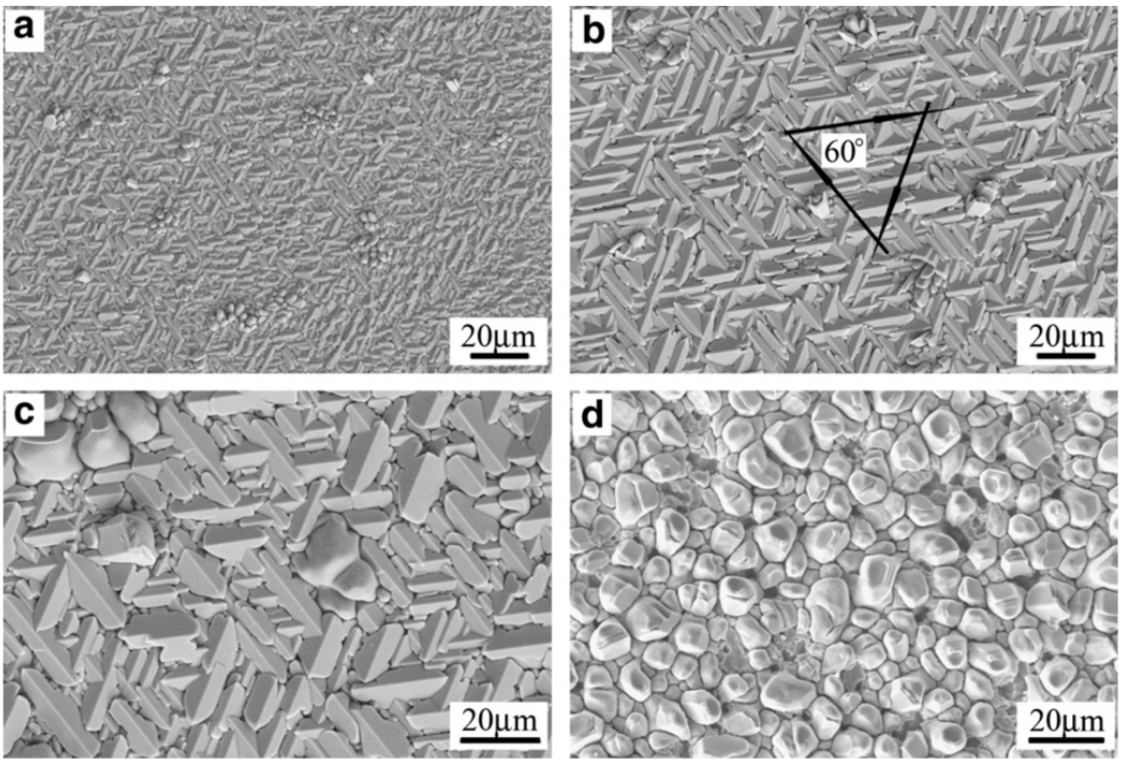

Fig.7 Cu_6Sn_5 grains morphologies formed on (111) Cu at 260 °C for (a) 5 s, (b) 60 s, (c) 320 s, and (d) 600 s [18]

IMC facets are also affected by substrate copper orientation. It is widely believed that there are certain orientation relationships between Cu_6Sn_5 IMC and substrate to reduce interfacial energy. Cu_6Sn_5 precipitate randomly on Cu during nucleation, and during growth period, scallops not following the orientation relationship will grow in a rather slow rate or be quickly consumed. As shown in Fig.7, Cu_6Sn_5 shows textured growth on (111) Cu single crystal for 5s. The faceted structure may not be able to last for a long reflow time, as the equilibrium structure is determined by interfacial energy rather than growth rate. In the literature review section, different Cu_6Sn_5 morphologies on different substrates would be discussed in details.

2. LITERATURE REVIEW

2.1 Orientation relationships between Cu_6Sn_5 and Cu

The structure of Cu_6Sn_5 has been widely studied due to the importance of Sn-based solder. There are two types of Cu_6Sn_5, high temperature η phase stable at T > 186 °C and low temperature η' phase stable when T < 186 °C. Most researchers assumed the IMC in as-soldered joints to be η phase Cu_6Sn_5, since the typical cooling time is insufficient for $\eta \rightarrow \eta'$ transition to take place in soldering process, and high-temperature η-Cu_6Sn_5 remains as a metastable phase [4]. Electron diffraction shows that both two IMC phases have monoclinic structure, but for η phase there is a strong pseudohexagonal symmetry around Cu atoms [20-23]. Therefore in literature most researchers took η -Cu_6Sn_5 as a hexagonal structure, and it is widely observed that the hexagonal Cu_6Sn_5 facets were elongated along [0001] direction, as shown in Fig. 5a. Furthermore, it has been found out that Cu_6Sn_5 hexagonal rods grew along [0001] direction with {10-10} side facets in liquid Sn-based solder [13,22]

Tu et al used micro-x-ray diffraction to study the morphology in high accuracy, and have discussed the relationship between monoclinic Cu_6Sn_5 and Cu substrate. They noticed [-101] direction of η phase tends to lay parallel to [110] direction in Cu substrate [19]. Considering the high pseudohexagonal symmetry, the [-101] direction of η is close to [0001] direction of hexagonal structure. As the IMC facets were elongated along [0001] direction, it indicates that the elongation direction of Cu_6Sn_5 grains is parallel to [110] direction of substrate. As shown in Fig.8, the [110] directions in a (001) single crystal Cu are in plane and perpendicular to each other. Consequently, IMCs on (001) Cu are elongated at perpendicular directions.

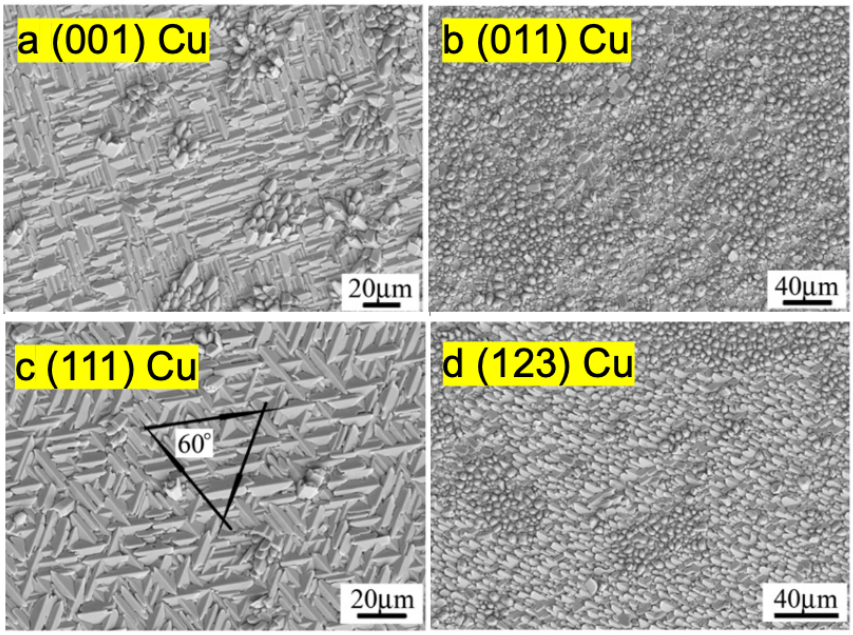

Fig. 8 SEM images of Cu_6Sn_5 on (a) (001) Cu, (b) (011) Cu, (111) Cu and (123) Cu after 30 s reflow. Faceted structures can be clearly observed for IMCs growing on (001) and (111) Cu, and there is a visible difference on IMC morphologies growing on different oriented substrate [20]

Additionally, though all Cu_6Sn_5 facets were aligned in a way that IMC [-101] direction is parallel to [110] direction in Cu substrate, six different crystal-plane relationships were observed:

$(001)_{Cu}$ // $(010)_{Cu6Sn5}$, $(001)_{Cu}$ // $(343)_{Cu6Sn5}$, $(001)_{Cu}$ // $(-3\ 4\ -3)_{Cu6Sn5}$

$(001)_{Cu}$ // $(101)_{Cu6Sn5}$, $(001)_{Cu}$ // $(141)_{Cu6Sn5}$, $(001)_{Cu}$ // $(-1\ 4\ -1)_{Cu6Sn5}$

Considering the hexagonal symmetry, (010), (343) and (-3 4 -3) planes in monoclinic Cu_6Sn_5 are close to {10-10} planes in hexagonal structure, and (101), (141), (-14-1) planes are close to {11-20} planes. The researchers believed the relationship between IMC and substrate is determined by minimum lattice mismatch, as misfit between the two phases is only 0.24% when [-101] direction of Cu_6Sn_5 is parallel to [110] of Cu.

Other researchers agreed on the minimum mismatch conclusion, but have proposed a new structure. Zou et al claimed that the IMCs should actually be low temperature η' phase (a = 11.022, b = 7.282, c = 9.827, β = 98.84°)[20]. They tried on more substrates and claimed four orientation relationships between IMC and Cu single crystal:

(001) Cu // $(010)_{Cu6Sn5}$, (001) Cu // $(102)_{Cu6Sn5}$, (111) Cu // $(010)_{Cu6Sn5}$, (111) Cu // $(102)_{Cu6Sn5}$

They also claimed that [110] and [-110] direction in (001) Cu are parallel to [-201] in Cu_6Sn_5, and [1-21],[-1-12],[-211] direction in (111) Cu are parallel to [-201] in Cu_6Sn_5. They attributed the substrate/IMC relationship to the fact that misfit between [-201] direction of Cu_6Sn_5 and <110>,<11-2> directions of Cu is 0.32% [20]. Impressive and enlightening as the results were, based on the TTT diagram in Ref [4], most soldering process would not have such a slow cooling rate to form η', so the conclusion itself is not very useful.

There is also different explanation for the substrate/IMC relationship rather than minimum lattice mismatch theory. Yang et al pointed out that kinetic factor as maximum rate of free energy changes is determinant of Cu_6Sn_5 facet crystal planes. As shown by the EBSD results in Fig.9, they found out that there are two types of Cu_6Sn_5 hexagonal rods in supersaturated solder. When formed on (111) Cu single crystal, Cu_6Sn_5 roofs are composed of {11-20} side faces and {10-10} top faces. In comparison, on (001) Cu the side faces of IMC are {10-10} planes and top faces are {11-20} planes [24,25]. And the elongation direction of Cu_6Sn_5 is always along [0001] direction for both substrates, which is not necessarily the smallest mismatch directions. The researchers pointed out that both {11-20} and {10-10} have six-fold symmetry normal to [0001] direction, therefore the two set of crystal planes may be thermodynamically alternative. They noticed the similar orientation relationship as Tu et al [21] that [0001] direction of IMC is parallel to substrate <110>, while {11-20}//{112} and {10-10}//{111}.

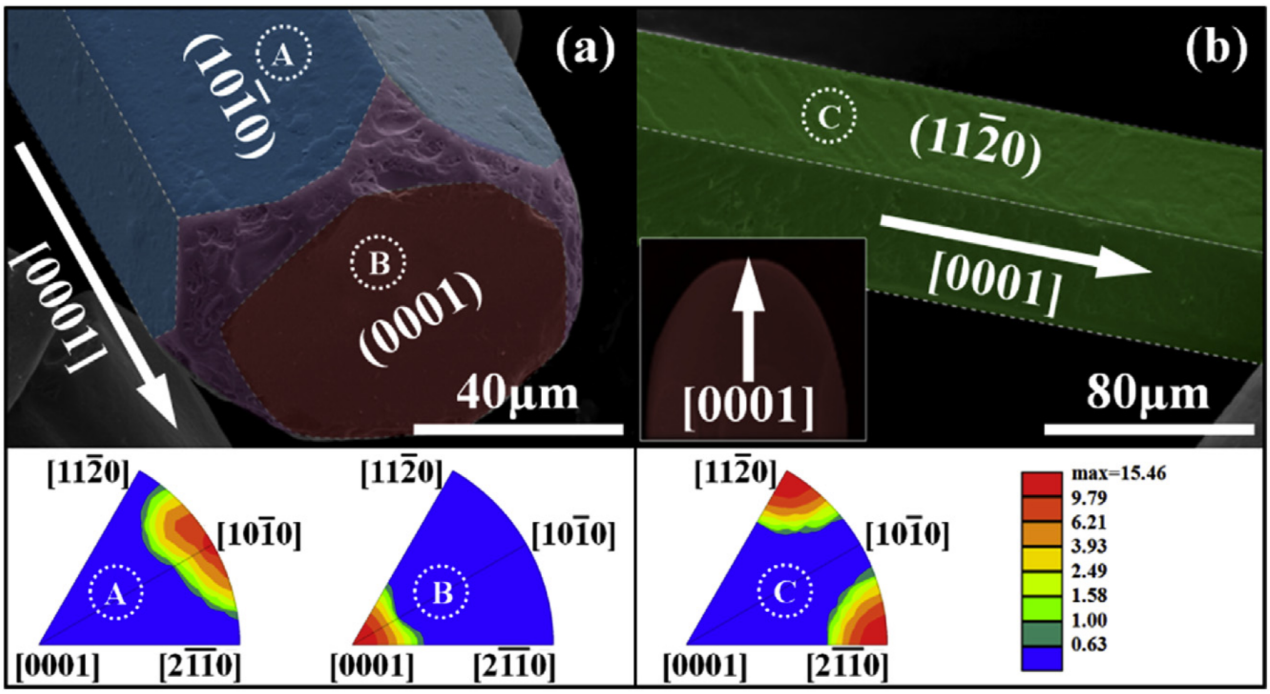

Fig. 9 EBSD detected crystal planes of two Cu_6Sn_5 IMCs. (a) truncated hexagonal rod with (10-10) side faces and (0001) end face and (b) anther hexagonal rod with (1120) side face and elongated along [0001] [25]

2.2 Summary

There are many literature reports focusing on the orientation relationships between Cu substrate and Cu_6Sn_5 facets. However, as introduced above, the ambiguity remained as different authors used different crystal structures and experiment methods. Different growth mechanisms have been proposed as well. For example, although most people agreed that the hexagonal IMCs grow by axial screw dislocation, some observed a solid-to-hollow transition in the hexagonal rods, and proposed that as IMC rods grow, the core was eventually wetted as the strain energy of the dislocation core exceeds certain limit. [13]

Therefore, we designed our experiment on large-grain polycrystalline Cu so that we can compare different substrate orientations and rule out other possible factors. The IMCs would be considered as η phase since it is almost impossible to obtain η' phase in typical cooling process. Furthermore, to better see the orientation relationship, hexagonal structure rather than monoclinic structure would be considered in the following sections due to the strong

pseudohexagonal symmetry, and an orientation relationship will be established between Cu substrate and Cu_6Sn_5. The relationship will then be presented with the help of inverse pole figure.

3. METHOD

Copper foil (99.9999%, Alfa Aesar) was cut into 10 mm*10 mm*1mm square pieces and were cleaned ultrasonically to remove surface contaminants. As shown in Fig.5, the average length of IMC should be no less than 10 μm so as to tell different morphologies apart. Therefore the minimum grain size of Cu substrate should be larger than 100 um to differentiate IMC grains. The cleaned Cu foils were annealed at 600 °C for 3 hours to obtain acceptable grain size, and then mechanically polished to remove oxide layer. After polishing, Cu foils were cleaned with running water, and each foil was etched with 5ml ammonium hydroxide, 0.3ml 50% hydrogen peroxide and 9.7 ml water for 1 minute. The foils were then cleaned with running water and ethanol to remove the residue etchant. The etched samples were observed using optical microscope to estimate the average grain size. The etching process performed is an efficient way to make sure Cu substrate has expected grain size.

Next, hardness tester was used to leave non-parallel indents on Cu foils in order to compare orientations between substrate and IMC in the following steps. Cu substrate was scanned with Quanta650 for EBSD analysis and inverse pole figures were obtained for the orientation distribution of Cu grains. Average grain size was automatically calculated by Team software and verified our observation from optical images of etched sample.

To form IMC on substrate, the substrate was gently polished again and cleaned with 50% diluted H_3P0_4 for a minute, and flux was then applied to improve wettability and remove oxide layer. Sn3Ag0.5Cu solder balls (diameter = 625 μm) were put on top of flux to form Cu_6Sn_5. The solder system was reflowed on a hot plate at 260°C for about 5s, 10s, 30s, 60s, 200s and 600s. It was observed that solder balls melted quickly and formed a cap during reflow. Two sets of sample were prepared for top-view and cross-section images respectively. For top-view samples solder cap was first partially removed by mechanical polishing, and then selective etching using 37% HCl solution for 30 minutes. For cross-section images samples were mounted into epoxy and polished.

After IMC formation, the sample was again observed with Quanta for SEM images to study IMC morphology and growth rate. Average IMC thickness was measured using ImageJ, and

random test lines were put on the image to measure the average intersection. The average grain size in top-view samples were used to verify the as-calculated average thickness in cross-section samples.

Since EBSD has a high demand on surface flatness, it is not easy to obtain IMC orientation directly from EBSD analysis. But a relationship between IMC and underlying substrate can still be built by locating the indents after Cu_6Sn_5 formation and comparing the morphology with literature reports. To build the quantitative relationship between IMC and substrate orientation, point analysis was taken to obtain the orientation information on both Cu side and IMC side in cross-section. An orientation relationship was built between IMC and underlying Cu substrate, and was visualized using an inverse pole figure.

4. RESULTS

4.1 Growth rate

Cu substrate with large grains was obtain after annealing, and piranha solution was chosen as an etchant for observation using optical microscopes. Fig. 10 is an optical image of the after-annealed substrate. Based on literature result in Fig.8 (b) and (c), the average thickness of Cu_6Sn_5 facets is 3-5 μm. Therefore the average size of underlying Cu grains should be no less than 100 μm in order to have adequate amount of facets on different oriented Cu grains.

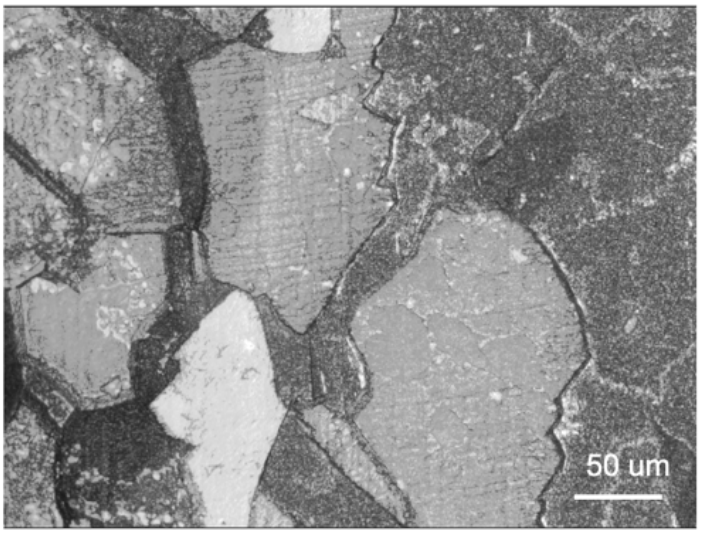

Fig. 10 optical image of after-annealed Cu substrate etched by piranha solution

Different samples were prepared for different reflow time. As seen in Fig.11 at 5s a continuous Cu_6Sn_5 layer was already formed at the interface. IMC has most irregular shapes at 30s, which may correspond to anisotropic faceted growth, and the morphology turned to more rounded scalloped structure when reflow time is longer than 60s. The average thickness of IMC increases with longer reflow time, and was quantitatively analyzed by measuring the intersection of IMC layer with parallel test lines. 20 perpendicular test lines were used for each sample during analysis, and error bars were introduced in the thickness – $time^{1/2}$ plot as shown in Fig. 12 (a).

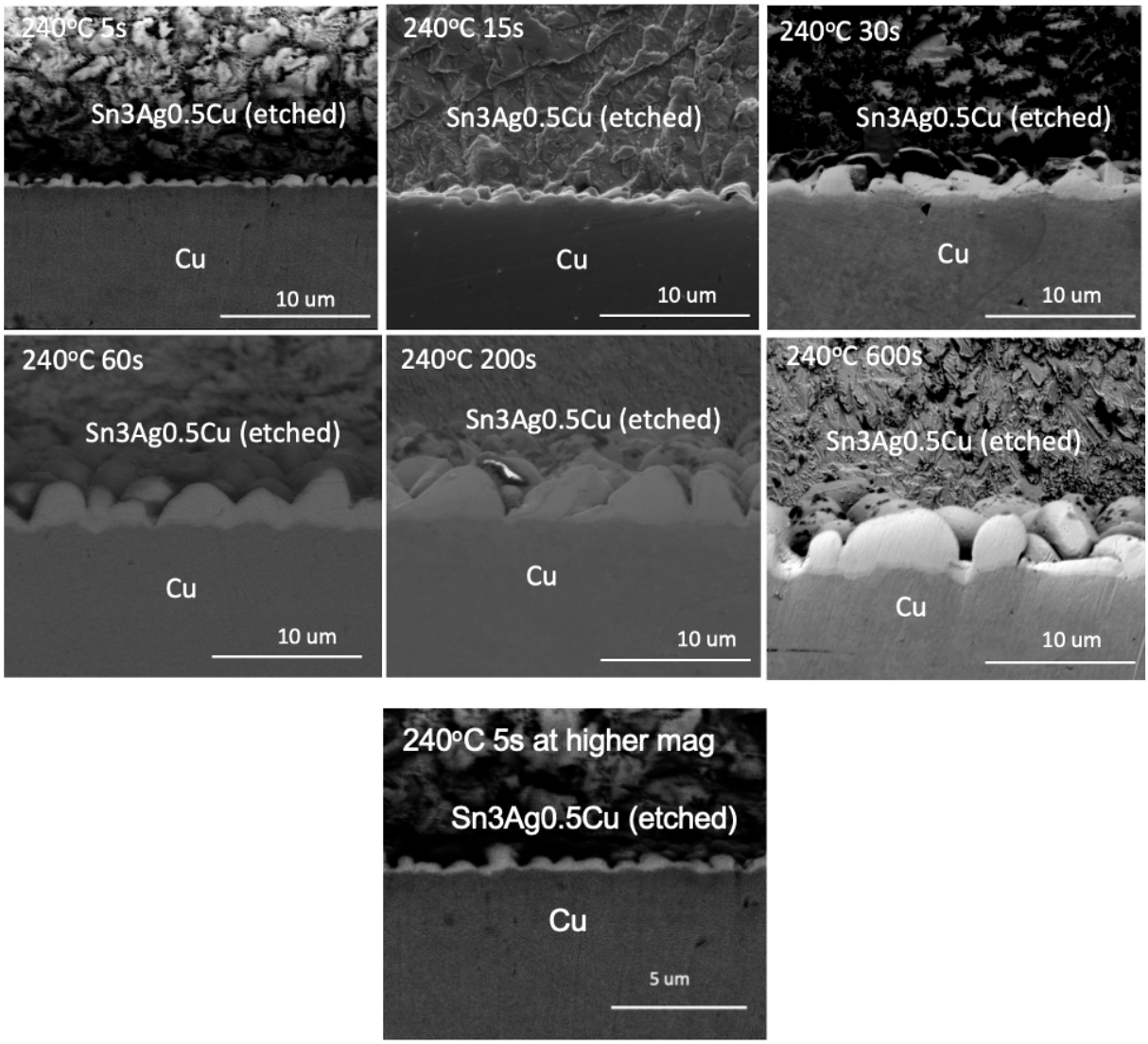

Fig. 11 cross-section images of Cu_6Sn_5 formed for different amount time

Average thickness was first fitted based on parabolic diffusion law as shown in Fig.12 (a). However, when annealing time is longer than 60s ($t^{1/2} = 7.75$), linear fitting for thickness - $t^{1/2}$ is not very successful and more likely to be a piecewise function. The two separate functions can be better observed when thickness was plotted into ln(thickness) – ln(time), in which the slope corresponds to growth exponent n. When annealing time is less than 60s, n = 0.6; when annealing time is greater than 60s, n = 0.26. The larger n is because at the very beginning IMC layer was relatively thin, and diffusion distance of Cu and Sn atoms was short enough that IMC growth was controlled by both reaction and diffusion. As reflow time increases, IMC layer became thicker and Cu_6Sn_5 grains became more rounded, and coarsening start to occur. In this

situation interfacial diffusion as well grain boundary diffusion was dominant over lattice diffusion , which lead to a growth exponent smaller than 0.5.

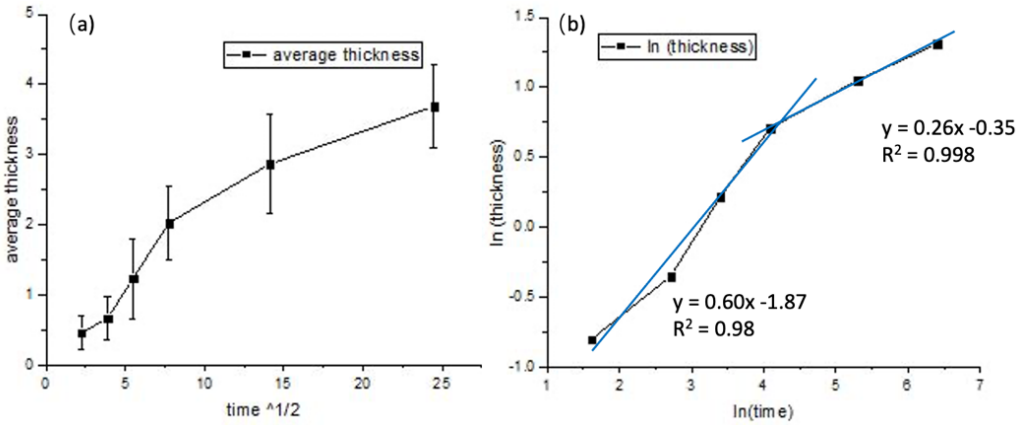

Fig. 12 cross-section images of Cu_6Sn_5 formed for different amount time

4.2 Morphology evolution

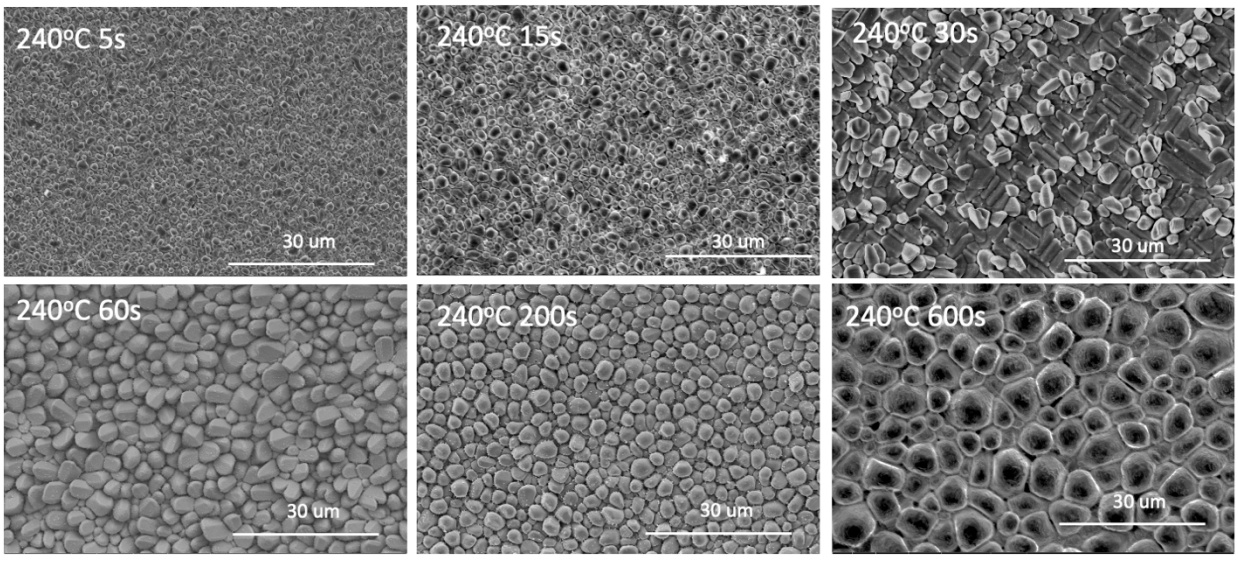

Fig. 13 top-view images of Cu_6Sn_5 formed for different amount time

Another set of samples were prepared for top-view images. Intersections of test line were measured similar to those cross-section samples so as to verify the results of average thickness obtained from the former samples. More importantly, morphology transition was observed at different reflow time. When reflowed for 5s, only small Cu_6Sn_5 grains was observed, most of

which had a small aspect ratio. When reflowed for 30s, anisotropic growth was clearly observed, and some Cu_6Sn_5 grains growing in plane were perpendicular to each other, similar to those found in literature [25]. At longer reflow time Cu_6Sn_5 grains became less faceted and more rounded. The top-view images matched well with cross-section ones, in which IMCs at 30s reflow time had most irregular shape, and the growth became less obvious as reflow time increases.

Based on the results from increased reflow time, the conclusion can be made that Cu_6Sn_5 facets, though had been observed by many researchers, should be a growth shape compared to equilibrium shape. The anisotropic structure is more likely to be caused by difference in growth rate for different directions, and at long enough time, at equilibrium the IMCs grains would transform into scallops due to ripening effect. As mentioned in the introduction part, the misuse of "equilibrium shape" and "growth shape" have been observed in many previous study, which is worth to clarify and emphasize. Equilibrium shape denotes the shape formed at equilibrium, which could be achieved after a long enough time; on the contrary, growth shape can be observed in a relative short time and may indicate an unstable structure. Equilibrium shape is the result of anisotropy in interfacial energy, while growth shape indicates a difference of growth rate for different crystal planes.

Additionally, round-shaped scallops formed at equilibrium indicates a relatively low IMC/solder interfacial energy, which only appears when broken bond energy is low at the interface. Atomically scallops would have many atomic steps and kinks at the surface with broken bonds to have a scallop structure, which implies a relatively low and isotropic interfacial energy. In comparison, based on the literature layered Cu_6Sn_5 was formed during aging when solder was in solid state, and scallop Cu_6Sn_5 would even transform into layered structure when temperature is below solder melting point [13,18]. The transformation may result from the fact that complete wetting condition ($2\sigma_{IMC\text{-}solder} < \sigma_{grain\ boundary}$, σ as the interfacial energy) is no longer true when solder is in solid state.

4.3 Orientation relationship

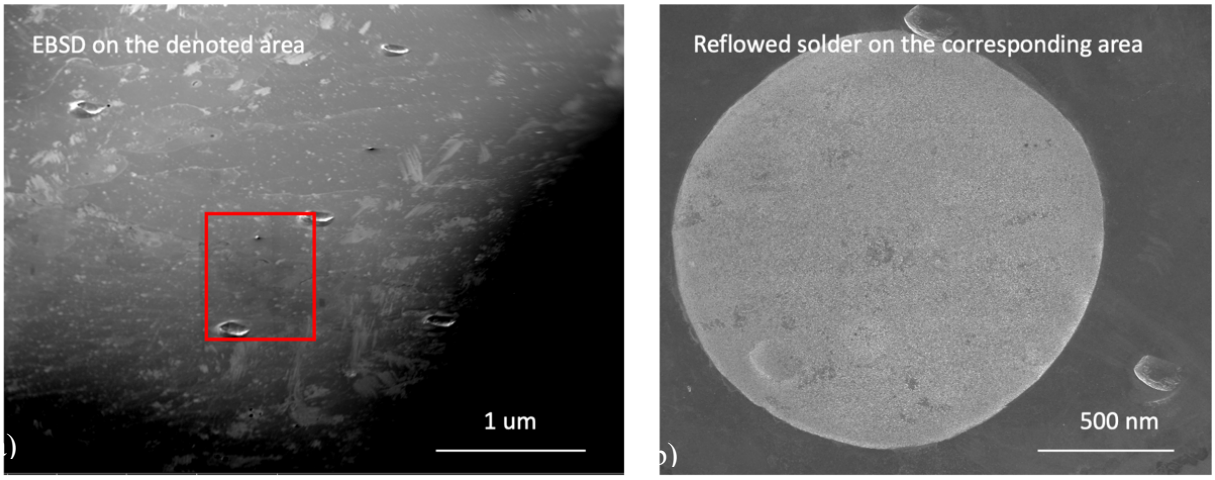

Fig. 14 SEM images (a) before and (b) after solder reacted with Cu substrate. EBSD analysis was performed on the circled area as denoted by the red rectangle in (a)

Orientation distribution of Cu substrate was analyzed using EBSD, and as shown in Fig.13, three indents were purposely designed not on a same line, and EBSD analysis was performed on the area circled out. Solder was later melted and reacted on the corresponding area with the help of indents location, so that the consequent IMC morphology can be compared with the previous ESBD results. IMC morphology was observed using SEM, and similar structures were noticed as ones shown in the literature. Additionally, the crystallographic information of IMC facets was analyzed on a cross-section sample as shown in Fig.14 in both Cu side and Cu_6Sn_5 tips, and orientation relationship between Cu substrate and IMC can be built by listing and comparing their crystal planes respectively.

The benefit of such experiment design is that a lot more crystallographic information can be collected and analyzed, not limited to some specific orientation like (001) and (111). Besides, IMC formation on a polycrystalline substrate helped rule out other possible factors, and in this situation conclusion can be made that substrate orientation was the only factor leading to different IMC morphology.

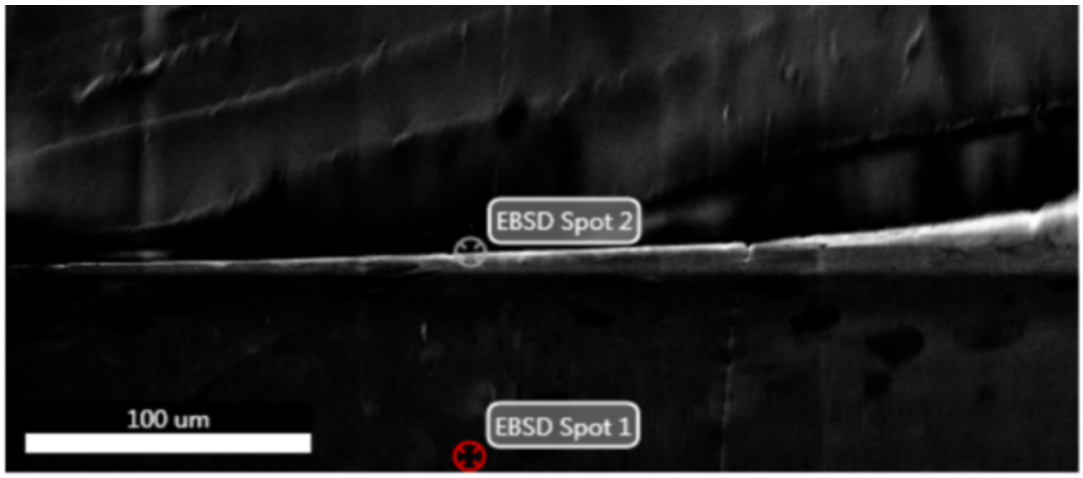

Fig. 15 Point analysis EBSD on both Cu substrate (spot 1) and IMC (spot 2). Same analysis were repeated several time to obtain the orientation relationship

5. DISCUSSION AND CONCLUSION

EBSD analysis for Cu substrate was performed first as discussed in previous section to obtain an orientation mapping. An example of Cu orientation was shown in Fig.16. To establish a complete orientation relationship between substrate and IMC, the crystallography information of Cu_6Sn_5 facets after reflow were again analyzed using EBSD. The analysis for Cu_6Sn_5 facet orientation was first performed on top-view samples, however the signal was quite low as EBSD has a high requirement on surface flatness. Polished cross-section samples were then analyzed to meet the flatness requirement, which is shown in Fig.16. As the average thickness of IMC facets was smaller than 2 μm, CI index in both measurement were not very high. Despite of the low CI value, several point analysis data were still able to be obtained from the cross section sample, and an orientation relationship can be built by comparing the crystal directions in Cu substrate and in Cu_6Sn_5.

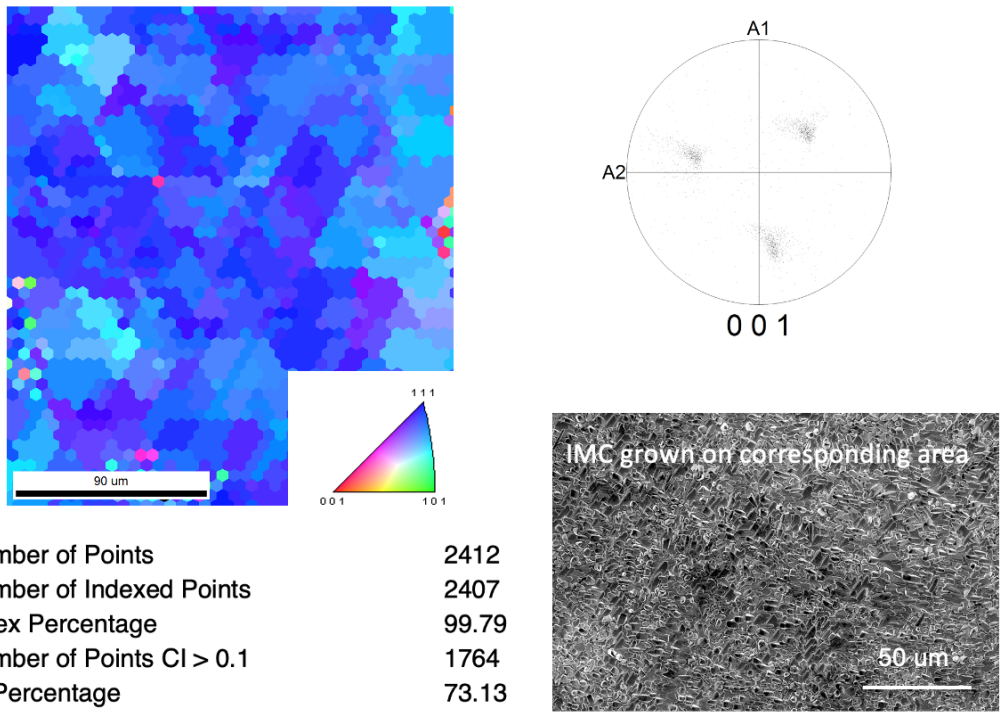

Number of Points	2412
Number of Indexed Points	2407
Index Percentage	99.79
Number of Points CI > 0.1	1764
CI Percentage	73.13

Fig. 16 EBSD pattern of Cu substrate (pole figure and inverse pole figure) and corresponding SEM images. Both the inverse pole figure (left) and the pole figure (top right) show that the major area were covered by (111) oriented Cu grains. SEM images were then taken for IMCs growing on the previously measured area

As shown in Fig. 16, Cu_6Sn_5 grains grew on (111) oriented Cu were elongated in plane and 60 degree from each other, same as those structures observed in literatures. Additionally, point analysis was performed using EBSD and the orientation relationship was summarized in an inverse pole figure as shown in Fig. 17. To develop a better idea about the relationship, the four Miller index were translated into three index for hexagonal Cu_6Sn_5, converting the coordinates in hexagonal systems into cartesian systems. And the rotation matrix R was calculated from observed direction (h k l) to (111) directions in Cu. After the calculation of R, it is multiplied with the observed Cu_6Sn_5 orientation to locate the after-rotation position of IMC orientation in Cu (111) pole figure.

The rotation matrix R is the product of g^{-1} and D, $R = G^{-1}*L$. G^{-1} is the rotation matrix from (h k l) to sample normal direction (ND), and L is the rotation matrix from ND to (111). G, the inverse of G^{-1}, can be expressed as

$$G = \begin{bmatrix} \cos\varphi_1 \cos\varphi_2 - \sin\varphi_1 \sin\varphi_2 \cos\Phi & \sin\varphi_1 \cos\varphi_2 + \cos\varphi_1 \sin\varphi_2 \cos\Phi & \sin\varphi_2 \sin\Phi \\ -\cos\varphi_1 \sin\varphi_2 - \sin\varphi_1 \cos\varphi_2 \cos\Phi & -\sin\varphi_1 \sin\varphi_2 + \cos\varphi_1 \cos\varphi_2 \cos\Phi & \cos\varphi_2 \sin\Phi \\ \sin\varphi_1 \sin\Phi & -\cos\varphi_1 \sin\Phi & \cos\Phi \end{bmatrix}$$

while $\varphi_1, \Phi, \varphi_2$ are the Bunge angles or Euler angles given by EBSD point analysis, and correspond to rotation angles around z axis, x axis, and z' axis. [26]

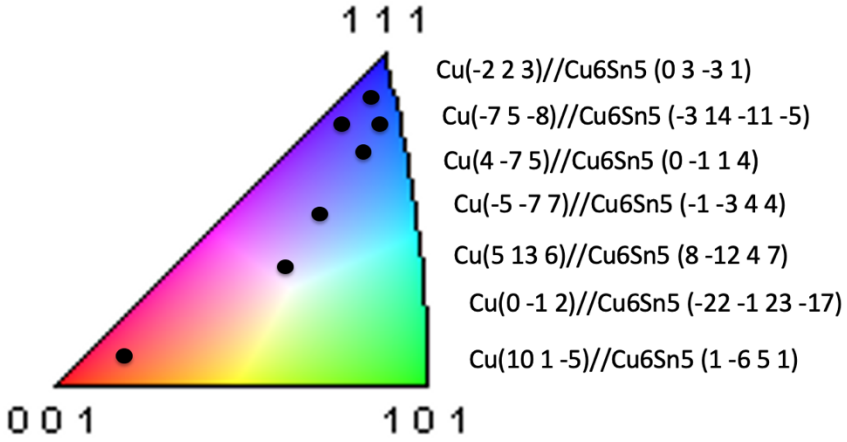

Fig. 17 orientation relationship between Cu substrate and Cu_6Sn_5 presented in a orientation triangle. The black dots indicate Cu orientation from the point analysis, and the crystallographic information of corresponding Cu_6Sn_5 are also included in the form of Cu //Cu_6Sn_5

Based on the rotation matrix calculation, it is observed that {111} planes in Cu tends to stay in parallel with {10-10} planes in Cu_6Sn_5, and {012} planes in Cu tends to stay in parallel with {10-11} planes in Cu_6Sn_5The microstructures match well with the conclusion as well. For Cu substrate shown in Fig.15, most areas are covered by (111) oriented grains, and IMC grains elongated in plane indicating that the normal vectors of most IMC grains should be {10-10} or {11-20}.

In conclusion, Cu_6Sn_5 facet formation identical to the literature was observed on polycrystalline Cu substrate at 240°C for 30s. Different reflow temperatures haven't been tried due to lack of time, but it worth trying as faceted structures were also discovered at higher temperature, like 260 °C [10,19]. Hot plate is chosen for the sample preparation, as the reflow time for typical reflow oven is too long for facets formation. However, in using hot plate the calibration is very important, and it is suggested to use thermocouples every time

before preparing samples. Interesting as the structures are, IMC facets are not equilibrium shapes and will be replaced by scallops after a long enough time.

Point analysis were performed on both Cu side and Cu_6Sn_5 side to establish the orientation relationship. A detailed explanation of EBSD was covered in this thesis and could serve as a good starting point for future work. To get more accurate crystallographic data from Cu substrate and Cu_6Sn_5 facets, further quantitative analysis may be required with better resolution and more strict requirement may be proposed for preparing EBSD samples to prevent drifting. In literature, researchers have used micro X-ray diffraction analysis to obtain orientation information from a selected area. An alternative way is to use AFM to get the height profile and calculate the tilting angle between Cu_6Sn_5 rods and substrate. Confocal microscopy may be another way to obtain the orientation map by analyzing 3D structure.

REFERENCES

[1] Laurila, T., V Vuorinen, and J. K. Kivilahti. “Interfacial reactions between lead-free solders and common base materials.” *Materials Science and Engineering: R: Reports*49.1-2 (2005): 1-60.

[2] Wang H, Ma X, Gao F, Qian Y. “Sn concentration on the reactive wetting of high-Pb solder on Cu substrate”. Materials chemistry and physics, 2006, 99(2-3): 202-205.

[3] Saunders, N., and A. P. Miodownik. "The Cu-Sn (copper-tin) system." Bulletin of Alloy Phase Diagrams 11.3 (1990): 278-287.

[4] Nogita, Kazuhiro, et al. "Kinetics of the η–η′ transformation in Cu_6Sn_5." *Scripta Materialia* 65.10 (2011): 922-925.

[5] Park, M. S., and R. Arróyave. "Early stages of intermetallic compound formation and growth during lead-free soldering." *Acta materialia* 58.14 (2010): 4900-4910.

[6] Hong, K. K., and Joo Youl Huh. "Phase field simulations of morphological evolution and growth kinetics of solder reaction products." Journal of electronic materials 35.1 (2006): 56-64.

[7] Gusak, A. M., and King-Ning Tu. "Kinetic theory of flux-driven ripening." *Physical Review B* 66.11 (2002): 115403.

[8] Suh, J. O., et al. "Size distribution and morphology of Cu_6Sn_5 scallops in wetting reaction between molten solder and copper.” Acta Materialia 56.5 (2008): 1075-1083.

[9] Gagliano, R. A., Gautam Ghosh, and M. E. Fine. "Nucleation kinetics of Cu_6Sn_5 by reaction of molten tin with a copper substrate." Journal of electronic materials 31.11 (2002): 1195-1202.

[10] Ma, H. R., et al. "Continuous growth and coarsening mechanism of the orientation-preferred Cu_6Sn_5 at Sn-3.0 Ag/(001) Cu interface." Materials Characterization 166 (2020): 110449.

[11] Yang, Ming, et al. "Cu_6Sn_5 morphology transition and its effect on mechanical properties of eutectic Sn-Ag solder joints." Journal of electronic materials 40.2 (2011): 176-188.

[12] Gagliano, Robert, and Morris E. Fine. "Growth of η phase scallops and whiskers in liquid tin-solid copper reaction couples." JOM 53.6 (2001): 33-38.

[13] J.W. Xian, S.A. Belyakov, M. Ollivier, K. Nogita, H. Yasuda, C.M. Gourlay. "Cu_6Sn_5 crystal growth mechanisms during solidification of electronic interconnections." *Acta Materialia*126 (2017): 540-551.

[14] Tu, King-Ning, Andriy M. Gusak, and M. Li. "Physics and materials challenges for lead-free solders." *Journal of applied Physics* 93.3 (2003): 1335-1353.

[15] Choi, Won Kyoung, et al. "Grain morphology of intermetallic compounds at solder joints." Journal of materials research 17.3 (2002): 597-599.

[16] Jackson, K. A. "Current concepts in crystal growth from the melt." Progress in solid state chemistry 4 (1967): 53-80.

[17] McQuarrie, Donald Allan, and John Douglas Simon. Physical chemistry: a molecular approach. Vol. 1. Sausalito, CA: University science books, Chapter 24, 1997.

[18] Gao, F., and T. Takemoto. "Effects of addition participation in the interfacial reaction on the growth patterns of Cu_6Sn_5-based IMCs during reflow process." *Journal of alloys and compounds* 421.1-2 (2006): 283-288.

[19] Nogita, Kazuhiro. "Stabilisation of Cu_6Sn_5 by Ni in Sn-0.7 Cu-0.05 Ni lead-free solder alloys." *Intermetallics* 18.1 (2010): 145-149.

[20] Zou, H. F., H. J. Yang, and Z. F. Zhang. "Morphologies, orientation relationships and evolution of Cu_6Sn_5 grains formed between molten Sn and Cu single crystals." Acta Materialia 56.11 (2008): 2649-2662.

[21] Suh, J. O., King-Ning Tu, and N. Tamura. "Preferred orientation relationship between Cu_6Sn_5 scallop-type grains and Cu substrate in reactions between molten Sn-based solders and Cu." *Journal of Applied Physics* 102.6 (2007): 063511

[22]Suh, Jung-Ook, King-Ning Tu, and Nobumichi Tamura. "Dramatic morphological change of scallop-type Cu_6Sn_5 formed on (001) single crystal copper in reaction between molten SnPb solder and Cu." Applied Physics Letters 91.5 (2007): 051907.

[23] Larsson, A-K., L. Stenberg, and S. Lidin. "Crystal structure modulations in η-Cu_5Sn_4." Zeitschrift für Kristallographie-Crystalline Materials 210.11 (1995): 832-837.

[24] Z.H. Zhang, H.J. Cao, H.F. Yang, M.Y. Li, and Y.X. Yu. "Hexagonal-rod growth mechanism and kinetics of the primary Cu_6Sn_5 phase in liquid Sn-based solder." Journal of Electronic Materials 45.11 (2016): 5985-5995.

[25] Zhang, Z. H., M.Y. Li, Z.Q. Liu, S.H. Yang. "Growth characteristics and formation mechanisms of Cu_6Sn_5 phase at the liquid-Sn0. 7Cu/(111) Cu and liquid-Sn0. 7Cu/(001) Cu joint interfaces." *Acta Materialia*104 (2016): 1-8.

[26] Depriester, Dorian. "Computing Euler angles with Bunge convention from rotation matrix." (2018).